Published in final edited form as:

Nat Chem Biol. 2015 August ; 11(8): 598–605. doi:10.1038/nchembio.1840.

Control of carotenoid biosynthesis through a heme-based *cis-trans* isomerase

Jesús Beltrán[1,2], **Brian Kloss**[3], **Jonathan P. Hosler**[4], **Jiafeng Geng**[5,9], **Aimin Liu**[5], **Anuja Modi**[6], **John H. Dawson**[6], **Masanori Sono**[6], **Maria Shumskaya**[1], **Charles Ampomah-Dwamena**[1,7], **James D. Love**[3,8], and **Eleanore T. Wurtzel**[1,2,*]

[1]Department of Biological Sciences, Lehman College, The City University of New York, 250 Bedford Park Blvd. West, Bronx, NY 10468

[2]The Graduate School and University Center-CUNY, 365 Fifth Ave., New York, NY 10016-4309

[3]New York Structural Biology Center, 89 Convent Avenue, New York, NY 10027-7556

[4]Department of Biochemistry, University of Mississippi Medical Center, 2500 N. State St., Jackson, MS 39216-4500

[5]Department of Chemistry, Georgia State University, 50 Decatur St. SE, Atlanta, Georgia 30303-2924

[6]University of South Carolina, Department of Chemistry and Biochemistry, 631 Sumter Street, Columbia, SC 29208-0001

Abstract

Plants synthesize carotenoids essential for plant development and survival. These metabolites also serve as essential nutrients for human health. The biosynthetic pathway leading to all plant carotenoids occurs in chloroplasts and other plastids and requires 15-cis-ζ-carotene isomerase (Z-ISO). It was not certain whether isomerization was achieved by Z-ISO alone or in combination with other enzymes. Here we show that Z-ISO is a *bona fide* enzyme and integral membrane protein. Z-ISO independently catalyzes the *cis*-to-*trans* isomerization of the 15–15′ C=C bond in 9,15,9′-*cis*-ζ-carotene to produce the substrate required by the following biosynthetic pathway

*Corresponding author: Dr. Eleanore Wurtzel, Department of Biological Sciences, Lehman College, The City University of New York, 250 Bedford Park Boulevard West, Bronx, NY 10468, Tel.: 718-960-8643; Fax: 718-960-8236, wurtzel@lehman.cuny.edu.

[7]present address: The New Zealand Institute for Plant and Food Research Limited, Private Bag 92 169, Auckland 1142, New Zealand

[8]present address: Albert Einstein College of Medicine, 1300 Morris Park Ave, Bronx, NY, 10461

[9]present address: School of Chemistry and Biochemistry, Georgia Institute of Technology, 315 Ferst Drive, Atlanta, GA 30332-0363

AUTHOR CONTRIBUTIONS

Wet lab experiments were performed by: Jesús Beltrán (cloning, protein expression, enzyme assays, HPLC, carotenoid analyses, mutagenesis, heme assays, UV-Vis spectroscopy), Brian Kloss (cloning, protein expression), Jonathan P. Hosler (ICP-OES, UV-Vis spectroscopy, heme assays, CO binding). EPR experiments were formed by Jiafeng Geng, and Aimin Liu. MCD experiments were performed by Anuja Modi, Masanori Sono, and John Dawson. Localization and import, including related gene cloning, was conducted by Maria Shumskaya. Jesús Beltrán and Eleanore T. Wurtzel performed bioinformatic analyses. Charles Ampomah-Dwamena prepared mutant Z-ISO fusion proteins while on a short-term sabbatical in the Wurtzel lab. All authors contributed to data analysis and to the writing and editing of the manuscript.

COMPETING FINANCIAL INTERESTS STATEMENT

The authors have no competing interests that might influence results and/or discussion in this manuscript.

enzyme. We discovered that isomerization depends upon a ferrous heme *b* cofactor that undergoes redox-regulated ligand-switching between the heme iron and alternate Z-ISO amino acid residues. Heme *b*-dependent isomerization of a large, hydrophobic compound in a membrane is unprecedented. As an isomerase, Z-ISO represents a new prototype for heme b proteins and potentially utilizes a novel chemical mechanism.

INTRODUCTION

Carotenoids constitute a large class of isoprenoids synthesized by all photosynthetic organisms, some bacteria, fungi, and arthropods[1]. Global vitamin A deficiency in children has sparked world-wide efforts to increase the levels of provitamin A carotenoids in food crop staples[2]. This goal rests on furthering knowledge of how plants control and biosynthesize carotenoids that can be converted in humans to vitamin A. Metabolic engineering and breeding of plants rich in particular carotenoids will continue to be an important objective for addressing the challenges of food security in a changing climate. Carotenoid functions are central to plant growth and development. The plant carotenoid biosynthetic pathway is mediated by nuclear-encoded enzymes localized to chloroplasts or other plastids[1,2]. The carotenoid biosynthetic reactions begin with formation of the colorless 15-*cis* phytoene, which undergoes desaturation and isomerization of double bonds to create carotenoids with yellow, red, and orange colors. The pathway requires an electron transfer chain and plastoquinones to channel electrons/protons produced during desaturation mediated by phytoene desaturase (PDS) and ζ-carotene desaturase (ZDS). PDS produces 9,15,9′-tri-*cis*-ζ-carotene, which must be isomerized at the 15–15′ *cis* C=C bond to form 9,9′-di-*cis*-ζ-carotene, the substrate for a second desaturase, ZDS (Fig. 1a). Although light can partially mediate this *cis* to *trans* C=C isomerization reaction, 15-*cis*-ζ-carotene isomerase (Z-ISO)[3,4] is essential, especially in tissues without light exposure, such as the endosperm tissue targeted for improvement of provitamin A carotenoids to alleviate global vitamin A deficiency[2]. Plants with insufficient Z-ISO also grow poorly under the stress of fluctuating temperature[5]. Since climatic variations alter the need for photosynthetic and nonphotosynthetic carotenoids, Z-ISO facilitates plant adaptation to environmental stress, a major factor affecting crop yield. Thus, Z-ISO is essential for maximizing plant fitness in response to environmental changes and for promoting accumulation of provitamin A carotenoids in edible tissues.

Mutants blocked in Z-ISO function accumulate 9,15,9′ tri-*cis*-ζ-carotene, the putative Z-ISO substrate[3]. When the *Z-ISO* gene is introduced into *E. coli* cells producing 9,15,9′ tri-*cis*-ζ-carotene, this carotenoid is isomerized into the putative Z-ISO product, 9,9′-di-*cis*-ζ-carotene[3]. These data suggest that Z-ISO is required for isomerization of the 15-*cis* bond in 9,15,9′-tri-*cis*-ζ-carotene but not the 15-*cis* bond in 15-cis phytoene. In *E. coli* experiments, the isomerization activity associated with Z-ISO occurs in the presence of several upstream carotenoid biosynthetic enzymes needed to produce the Z-ISO substrate. Thus, there remains the possibility that Z-ISO is not an independently-acting enzyme but instead alters one of the other enzymes present in order to gain a catalytic function of isomerization. Here we present data to demonstrate that Z-ISO is a *bona fide* enzyme that catalyzes isomerization through a

unique mechanism requiring a redox-regulated heme cofactor. This discovery raises new questions regarding control of carotenogenesis in plants.

RESULTS

Expression, isolation, and activity assays of Z-ISO

To directly test whether Z-ISO was a *bona fide* enzyme, we developed an *in vitro* assay using isolated Z-ISO from *Zea mays* and artificial liposomes containing the Z-ISO substrate. First, the substrate was purified from *E. coli*[3] and combined with lipids to form artificial liposomes. Next, we over-expressed and purified Z-ISO as a TEV protease-cleavable, maltose binding protein (MBP) fusion (MBP::Z-ISO) (Supplementary Results, Supplementary Fig. 1a and 1b). Lastly, the isolated fusion protein of 90% purity (Supplementary Fig. 1b) was incubated with TEV protease to cleave Z-ISO away from the fused MBP, prior to initiation of the isomerization reaction. As shown in Fig. 1b, conversion of the substrate to product occurred only in the presence of Z-ISO that had been pretreated with dithionite to a final concentration of 10 mM to create reducing conditions. The as-purified enzyme (considered to be oxidized), as well as heat denatured Z-ISO, were not functional. Therefore Z-ISO catalyzed isomerization only when the reaction was conducted under reducing conditions but not oxidizing conditions. The liposomes used for the *in vitro* assay were also essential, as reactions lacking liposomes did not work (data not shown)

Predicting Z-ISO structure and localization

To gain insight into the mechanism of isomerization, we sought to identify catalytic motifs or other characteristic domains in Z-ISO. Our previous BLAST[6] analysis suggested that although Z-ISO is highly conserved in plants, it only shares sequence homology (~76% similarity) with NnrU, an uncharacterized membrane protein associated with nitric oxide metabolism in noncarotenogenic bacteria that perform denitrification[3]. In addition, a chloroplast targeting sequence was identified in Z-ISO, suggesting that Z-ISO is a plastid-localized protein[3]. No other motifs could be identified to suggest a mechanism for isomerization. Therefore, we used bioinformatic approaches to generate hypotheses on the location and function of Z-ISO that were tested further.

MEMSAT3[7] predicted seven TM domains in maize Z-ISO (Fig. 1c) with TM 2–7 showing homology to the corresponding TM domains in NnrU[3]. In comparison to a functional Arabidopsis transcript (*ZISO1.1*), a shorter Arabidopsis transcript (*ZISO1.2*)[3] encodes a nonfunctional protein with one less TM domain at the C-terminus. The effect of the deletion suggests that the C-terminal TM domain is important for the function (e.g. activity or proper folding) of Z-ISO.

To test the prediction that Z-ISO is targeted to the chloroplast, we fused the gene encoding green fluorescent protein (GFP) downstream of the gene encoding Z-ISO, including its transit peptide. The fusion construct was then transiently expressed in maize leaf protoplasts. GFP fluorescence confirmed that Z-ISO co-localized in the chloroplast together with chlorophyll (Fig. 1D). *In vitro* chloroplast protein import demonstrated that Z-ISO is a chloroplast integral membrane protein (Supplementary Fig. 1a), as predicted by the topology

predictions. Taken together, our observations suggest that Z-ISO is localized in chloroplast membranes. We also found that Z-ISO exists in a high molecular weight protein complex of about 480 kDa (Supplementary Fig. 1b) as similarly noted for other carotenoid enzymes[8].

Next, we applied homology modeling tools to look for structural homologies missed by the BLAST analysis. We expected that homology modeling would be limited by the underrepresentation of membrane protein structures in the Protein Data Bank due to inherent difficulties in crystallizing membrane proteins. Homology modeling of Z-ISO using the Meta Server[9] program modeled the residues of Z-ISO onto an integral membrane protein, the diheme cytochrome *b* subunit of quinol:fumarate oxidoreductase[10]. The fold recognition program LOOPP[11] predicted that Z-ISO might contain nonheme iron (see below). These programs are based on unique algorithms and therefore the templates chosen for modeling by the programs were different. However, neither NnrU nor Z-ISO had been annotated as metalloproteins.

Detection of iron in Z-ISO

To test the prediction that Z-ISO is a metalloenzyme, inductively coupled plasma optical emission spectrometry (ICP-OES) was used to measure the metal content (Online Methods). The result showed that iron is present in the MBP::Z-ISO fusion, but not Ca, Cu, Ni, Mg, Mn, Mo or Zn. Since MBP is not a metalloprotein, the protein-bound iron was postulated to be exclusively associated with Z-ISO. Cultures with MBP::Z-ISO are brown (Supplementary Fig. 3a), as is the purified protein (Supplementary Fig. 3b), consistent with the presence of heme or nonheme iron.

To test specifically for heme, MBP::Z-ISO and cleaved Z-ISO and MBP were separated by SDS-PAGE and stained for heme[12] and then for total protein. The results showed that both MBP::Z-ISO and Z-ISO contained heme, while MBP did not (Fig. 2a and Supplementary Fig. 4). We next conducted a pyridine hemochrome assay to examine the heme cofactor independent of Z-ISO, and found that it is a heme *b* on the basis of the spectroscopic signature[13] (Fig. 2b). We also found that the related NnrU protein contains a heme *b* (Supplementary Fig. 5). Ultraviolet-Visible (UV-Vis) absorption spectroscopy (Fig. 2c) of as-purified Z-ISO, together with its bound heme, indicated the presence of an oxidized, ferric Fe(III) state, heme. To generate the spectrum of the reduced Z-ISO heme (with a ferrous, Fe(II), heme iron), the as-purified Z-ISO was treated with dithionite. The spectrum of the dithionite-reduced Z-ISO (Fig. 2c) is similar to those of cytochromes containing heme *b* with two axial histidine ligands[14]. Carbon monoxide (CO), was used as a diagnostic probe to test whether the heme could coordinate electrons with an exogenous ligand. The shift in the UV-Vis spectrum attributed to the heme indicated that CO could bind and coordinate to the heme iron of Z-ISO (Fig. 2c and 2d). The binding was stoichiometric given that the absorbance associated with CO binding was almost equivalent to that associated with the reduced heme. That is, the absorbance of the α band trough at 560 nm in the CO difference spectrum (Fig. 2d) was ~90% the intensity of the α band peak for the same sample in the reduced *minus* oxidized spectrum. The comparison indicated that at least 90% of the reduced heme had bound CO. This result suggested that one of the axial amino acid ligands may be displaced by an exogenous ligand. The significance of this observation is that the Z-ISO

heme iron may not be limited to shuttling electrons as in the case of hemes that participate in electron transfer, but instead the Z-ISO heme iron may serve a role in catalysis.

UV-Vis absorption spectroscopy analysis showed that an exogenous ligand can bind to the heme iron in the Fe(II) state but it was not known whether an exogenous ligand can displace an axial ligand when the heme is in the Fe(III) state. To test this possibility we introduced cyanide (CN^-), which is known to bind preferably to ferric rather than ferrous heme[15]. CN^- was added to both the as-purified enzyme with oxidized Fe(III) (ferric) heme and to the dithionite-reduced enzyme carrying a reduced Fe(II) (ferrous) heme, and the UV-Vis absorption was measured as shown in Fig. 2e. Binding of CN^- to the Fe(III) heme of Z-ISO using saturating concentrations of KCN was observed as indicated by the shift in the Soret peak (from 413 to 415/416 nm), and the new spectrum resembled that of cyanomyoglobin which has histidine as the protein-anchoring or so-called proximal ligand[16]. However, binding of CN- to the ferric iron was substoichiometric, based on analysis of the difference spectra. Addition of CN^- to the ferrous enzyme showed no spectral change (Supplementary Fig. 6), as expected[15]. These results support the presence of a pentacoordinate, high spin mono-His liganded ferric heme (in equilibrium with low spin hexacoordinate heme) which can bind exogenous ligand in the oxidized, inactive enzyme. The sub-stoichiometric binding of CN^- suggests that this pentacoordinate, high-spin species represents a small subset of the total ferric heme.

Detection of multiple heme species in Z-ISO

An X-band electron spin resonance (EPR) spectrum of the as-purified MBP::Z-ISO fusion protein indicated the presence of a high-spin ferric heme (i.e. heme *b* with an axial histidine ligand) at $g = 5.8$ and multiple low-spin hemes with broad EPR signals (Fig. 3a and 3b and Supplementary Table 1). In addition, a minor nonheme iron species was observed at $g = 4.3$ and is postulated to be non-specifically bound to Z-ISO. As summarized in Supplementary Table 1, the low-spin heme EPR signals shown in Fig. 3a and 3b are consistent with the existence of two major types of low-spin heme species with either a *bis*-His or His-Cys axial ligand set, respectively. The low-spin species at $g = 2.98$ is assigned as a hexacoordinate heme with a *bis*-His axial ligand set, based on the similarity of its *g*-factors to those of other heme species with a *bis*-imidazole axial ligand set[17,18]. The signals at $g = 2.54$, 2.50, and 2.43 are attributed to the g_x tensors for multiple components of a hexacoordinate low-spin heme species with a His-Cys axial ligand set[19,20]. Such low-spin species typically display a narrow distribution of the *g* factors, due to pronounced delocalization of the spin density to the cysteine ligand. The heterogeneity of this His-Cys coordinated heme species is likely originated from variations in the coordination position as well as the protonation or hydrogen-bonding state of the cysteine ligand. Previous studies on other systems have demonstrated that the *g* factors for His-Cys coordinated heme species are sensitive to the electronic properties of the heme environment and the protonation state of the axial ligands[19]. Next, the as-purified sample was chemically reduced with dithionite and the reduced sample was EPR silent (Fig. 3c). With addition of nitric oxide (NO), a strong EPR signal at the $g = 2$ region was detected (Fig. 3d), and is attributed to the formation of a low-spin hexacoordinate Fe(II)-nitrosyl heme complex[21]. NO binding is consistent with the finding that reduced MBP::Z-ISO also binds CO (Fig. 2c and 2d). The EPR spectrum of the

Fe(II)-nitrosyl complex of MBP::Z-ISO is similar to other Fe(II)-nitrosyl adducts of histidine-ligated hemes, such as those reported in cytochrome *c* oxidase, cytochrome *c* peroxidase, heme oxygenase, hemoglobin, myoglobin, and horse radish peroxidase[22,23], suggesting that a histidine residue is retained as the axial ligand of the ferrous heme when NO is bound.

EPR analysis revealed high-spin and low-spin hemes. A high spin heme can have an easily observable EPR signal, even if it is a minor component. To further examine the heme(s) in the same sample as used for EPR, we utilized magnetic circular dichroism (MCD) which detects mainly the heme chromophore (300 – 700 nm). To ascertain a detection limit of the percentage of high spin heme in a sample containing a mixture of low spin and high spin heme, we compared the MCD and UV-Vis absorption spectra of Fe(III) Cyt. *b*5 (100% low spin species)[24] and Fe(III) Mb (met-aqua-Mb) (~100% high spin)[25] in a series of low spin/high spin mixtures (95/5, 90/10, 80/20 and 50/50) (Supplementary Fig. 7). We concluded that Fe(III) Z-ISO (Fig. 4a) contains <20% (probably <10%) high spin heme at ambient temperature, presumably from equilibrium dissociation of an axial ligand from the low spin heme.

Z-ISO has only one heme with reversible His and Cys ligands

MCD also showed that ferric Z-ISO has two ligand pairs (His/His and His/Cys), consistent with the EPR results. This finding was determined by comparing the as-purified Z-ISO spectrum with that of a simulated mixture of Cyt. *b*5 (*bis*-His)[25] and imidazole (Im)-bound $P450_{CAM}$ (His-Cys)[26,27] (Fig. 4b). The data show a good fit to two ligand coordination modes in low spin ferric Z-ISO at a ~1:1 ratio. If there is only one heme center in the protein, His and Cys might occupy the distal side of the heme as alternative ligands while the proximal side is ligated by a common His. We also examined the MCD spectrum of the dithionite-reduced Z-ISO. MCD showed a single heme species in the reduced Z-ISO coordinated by *bis*-His (Fig. 4b). Importantly, the amount of reduced His/His heme was equivalent to the combined concentration of the His/His and His/Cys heme seen in oxidized Z-ISO.

If two heme centers exist, there should be two separate proximal histidines. To distinguish between these alternate hypotheses it was necessary to use another approach to identify all histidines in Z-ISO that could serve as heme ligands. We next searched for the specific residues that might function as Z-ISO heme ligands. We aligned available Z-ISO sequences, identified all evolutionarily conserved residues that have been reported to serve as heme ligands[28], mutagenized them to alanine, and tested for activity using *E. coli* complementation[3]. Of all conserved histidines, only two (H150, H266) were required for activity (Fig. 5a; Supplementary Table 2). Substitution with alanine at H150 (H150A) or H266 (H266A) decreased the conversion of the substrate to product as compared to wild-type Z-ISO. Loss of the isomerization activity was not due to absence of expression, the possibility of which was ruled out using an anti-maize Z-ISO polyclonal antiserum (Supplementary Fig. 8). Loss of either residue also disrupted heme-binding as evidenced by the reduction in bound heme for MBP fusion proteins carrying the alanine variants and by

the UV-Vis spectral shift seen for both the as-purified (oxidized) or dithionite-reduced proteins (Fig. 5b and Fig. 5c).

On the basis of the mutagenesis results, we were able to rule out the two-heme model for Z-ISO. Two hemes would have necessitated a total of at least three required histidines (two proximal and at least one distal), but we found no additional conserved histidines required for activity beyond H150 and H266 (Supplementary Table 2). Predicted locations of H150 and H266 based on the Z-ISO homology model (Fig. 6a) are consistent with coordination of a common cofactor. Therefore the data are consistent with the presence of a single heme that undergoes a change in axial ligation when reduced (Fig. 6b).

Does the heme ligand C263 function in isomerization?

The ability of Z-ISO to bind exogenous ligands indicates availability of an axial coordination site on its heme, and facile dissociation of one of two axial ligands. The most complete dissociation takes place in the reduced, active form of the enzyme. Z-ISO activity is predicated on the heme ligands H150 and H266 and on the heme iron being in the reduced state. Therefore, it is possible that the heme iron directly mediates isomerization by interacting with the substrate. An alternative hypothesis is that as a result of redox-dependent ligand switching, the switch to *bis*-His exposes C263 which becomes accessible to mediate catalysis. Precedence for the function of a Cys residue in catalysis, particularly in double bond isomerization, is seen for isopentenyl diphosphate (IPP) isomerase (IPPI), a nonheme enzyme that catalyzes double bond isomerization[29]. The C263 alternate heme ligand is the only cysteine in Z-ISO and it is evolutionarily conserved in all Z-ISO sequences. The Cys residue appears unlikely to function in protein dimerization as the *in vitro* reaction included the reducing agent, dithiothreitol, which would eliminate dimerization mediated by cysteine sulfhydryl bridges. If C263 is essential for catalysis, then mutagenesis to a non-redox active residue should inactivate the enzyme. As shown respectively in Fig. 5a and Supplementary Fig. 8, mutation to alanine had no effect on activity or expression, when using the *E. coli* complementation system. While the C263A MBP fusion variant carries a reduced amount of heme equivalent to the H266A variant, the UV-Vis spectrum of C263A is similar to that of wild type Z-ISO (Fig. 5b and 5c; Supplementary Table 3). Taken together, these results suggest that C263 is not catalytic but instead plays a role in heme binding and reversible heme ligation.

The heme is likely to function as the mechanistic cofactor based upon the observations that with loss of either of the apparent His ligands (H150 or H266) Z-ISO becomes inactive, the heme spectrum is altered and heme binding is reduced. EPR and MCD spectroscopy together identify the axial ligands as *bis*-His or His-Cys. It should be noted that H266 and C263 are only three residues apart. Therefore, these two residues are likely the labile ligands that can exchange with each other in the ferric state, whereas H150 is the tightly associated proximal ligand that always remains bound to the heme regardless of different redox or binding events (Fig. 6a and 6b). EPR spectra show a small amount of His-ligated, pentacoordinate, high-spin heme, a possible intermediate during the ligand exchange. The presence of this high-spin species with a coordination vacancy, in equilibrium with the two different hexacoordinate ligation states of the low-spin heme, is consistent with the

observation that CN^- can bind to the ferric heme of Z-ISO. Furthermore, the sub-stoichiometric binding of CN^- is consistent with the MCD calibration data (Supplementary Fig. 7) showing that the pentacoordinate, high-spin species is likely to be less than 10–20% of the total heme. When Z-ISO is reduced to the Fe(II) form, the heme ligand set becomes solely *bis*-His, suggesting a redox-dependent ligand switch. It is this reduced form that is active *in vitro*. The Fe(II) heme can bind NO and CO, which were used as diagnostic probes to experimentally interrogate the heme for available coordination sites needed to coordinate an exogenous ligand (Fig. 6b).

DISCUSSION

Z-ISO was shown to be an integral membrane isomerase that responds to redox state in performing a key step in carotenoid biosynthesis. Isomerization is dependent on a unique cofactor carried by Z-ISO, a heme that undergoes redox-dependent ligand switching. We propose that reduction of the heme iron switches coordination of the heme to *bis*-His and exposes the active site for substrate binding. In the proposed mechanistic model (Fig. 6c), binding of the Z-ISO substrate displaces the weakly associated H266 ligand, and the π electrons of the 15–15′ *cis* carbon-carbon double bond in the substrate serve as a Lewis base for coordination with the ferrous heme iron of Z-ISO. There is precedence for coordination between a carbon-carbon double-bond moiety and a heme iron as reported for a bacterial flavohemoglobin[30]. Spectroscopic evidence provides support for coordinate bonding between the iron of the histidine-coordinated heme and a carbon-carbon double bond of an unsaturated lipid. Binding to a transition metal such as iron can reduce the bond order of an alkene because the π electrons are delocalized into an empty orbital on the metal[31]. As a result of direct coordination between the ferrous heme iron of Z-ISO and the target double-bond in the substrate, the single sigma bond remaining in the substrate would be free to rotate to the energetically more favorable *trans* configuration, thus converting 9,15,9′-*cis*-ζ-carotene to 9,9′-*cis*-ζ-carotene. As a consequence of *cis* to *trans* isomerization, the entire structure of the 40-carbon ζ-carotene substrate would change from a bulky W-shape to a streamlined linear shape (Fig. 1a). These *cis* and *trans* geometrical isomers would interact uniquely with the microenvironment of the Z-ISO protein structure and contribute distinctly to membrane lipid fluidity. Therefore, it is predicted that the altered carotenoid structure would drive release of the product from Z-ISO, allowing further enzymatic conversions of the Z-ISO product by downstream enzymes. Notably, according to the hard-soft acid-base (HSAB) theory[32], Fe(II) is a soft Lewis acid compared to Fe(III), and thereby prefers ligation to soft Lewis bases. Given that the Z-ISO substrate is a soft Lewis base, it is anticipated that the ferrous state of Z-ISO presents superior binding kinetics and reactivity compared to the ferric state. In addition, coordination of the carotenoid double bond to the Fe(II) ion of the reduced Z-ISO heme forms a stable 18 e^- coordination complex. In contrast, an unsaturated and less stable (17 e^-) coordination complex would be generated if the substrate was coordinating electrons with the Fe(III) ion present in the as-purified Z-ISO heme. Thus, other than the aforementioned redox-dependent conformational changes, the HSAB analysis and the 18 e^- rule in organometallic chemistry further explain the molecular basis for redox control of the isomerization activity of Z-ISO.

Heme-dependent carbon-carbon double-bond isomerization is rarely reported in the literature. The only other double-bond isomerase known to utilize heme as a cofactor is a bacterial *cis-trans* fatty acid isomerase (CTI)[33]. CTI is a periplasmic enzyme that utilizes a *c*-type heme to perform a similar *cis* to *trans* isomerization of a double bond. However, little is known regarding the electronic structure or ligand coordination state of the heme iron in this enzyme. The hypothesized catalytic mechanism of CTI is distinct from that of Z-ISO. It is proposed that CTI functions in the oxidized ferric state and that the isomerization reaction is triggered by single-electron transfer from the double bond to the heme iron, oxidizing the double bond to single bond[33].

Our data show that reduction of the Z-ISO heme iron from Fe(III) to Fe(II) is necessary for enzyme activity. The heme reduction causes a ligand switch to *bis*-His and possibly triggers additional conformational changes at the active site of Z-ISO to allow substrate binding. In the resting ferric state, Z-ISO is postulated to be in a closed conformation, excluding the binding of the bulky substrate (Fig. 1a). Such redox-dependent ligand-switch phenomena have been observed in many other hemoproteins, and the purpose of the ligand-switch behavior is to induce conformational changes that drive functional activation. This strategy appears to be a common natural approach to control the functional activity of hemoproteins through redox changes. For example, cytochrome cd_1 nitrite reductase must be reduced to become catalytically active through a mechanism that involves a redox-mediated heme iron ligand switch[34]. Upon reduction, a tyrosine ligand of the d_1 heme in that enzyme is displaced to generate a coordinate vacancy for substrate binding. Similarly, the CO gas sensing transcription factor CooA contains a heme cofactor that undergoes a ligand switch in order for CooA to become competent for DNA binding[20]. Like Z-ISO, CooA goes through a redox-mediated ligand switch upon reduction of the heme iron; a cysteine axial ligand is replaced by a histidine, enabling the binding of CO to the heme iron at the ferrous state via displacement of the relatively weakly bound histidine ligand. Conformational changes then follow to drive DNA binding. Another example is bacterial di-heme cytochrome *c* peroxidase (bCcP)[35]. In the resting di-ferric state of bCcPs, one heme has a *bis*-His axial ligand set and the other heme has a His-Met axial ligand set. The two hemes are over 14 Å apart. A reductive activation process is generally needed for the proper function of bCcPs: single-electron reduction of the high-potential His-Met heme triggers a series of conformational changes that remotely displaces one of the histidine ligands of the other heme, allowing the access of the co-substrate, H_2O_2, to that site. Notably, a common feature of these examples is that reduction of the inactive ferric form generates the active ferrous form and the ligand switch as well as associated conformational changes enables the binding of substrate via the creation of a coordinate vacancy, a weakly associated ligand, or a binding cavity. This strategy can effectively protect the heme cofactor from non-productive binding events and thereby avoids undesired side reactions.

If the activity of Z-ISO is controlled by redox state, then how might plastid physiology and stress affect Z-ISO and downstream flux through the carotenoid pathway? Plastids undergo dramatic shifts in redox status as a result of photosynthetic activity in the light and nonphotosynthetic activity in the dark. It is known that changes in redox status are reflected through dynamic control of metabolism. For example, redox modulators (e.g. ferrodoxins

and thioredoxins) adjust heme and chlorophyll biosynthetic activity in response to varying redox state[36]. It has been proposed that carotenoid biosynthesis is also under redox control, although most of the molecular details are unknown[37]. It is already known that mutations that inhibit expression of Z-ISO will block production of carotenoid pathway end-products[3,4]. Based on the results presented here, we predict that changes in plastid redox state will directly influence Z-ISO activity, and as a consequence alter flux in the carotenoid biosynthetic pathway. Redox-tuning of Z-ISO activity could position Z-ISO as a gatekeeper for dynamic control of carotenogenesis on short time scales. That is, carotenoid pools could be rapidly adjusted by redox-tuning of Z-ISO to respond to variable needs for photosynthesis and signaling pathways related to stress and development.

Stress is a known factor affecting biosynthesis and action of carotenoids and their derivatives[38–41]. It is known that NO is produced directly at the site of carotenoid biosynthesis in plant plastids in response to stress[42] and has been shown to inhibit carotenoid accumulation[43]. NO is known to inhibit heme enzymes through binding to the heme iron[44], especially the ferrous form[45]. The ability of Z-ISO to bind NO, tested in the lab as a diagnostic heme ligand probe, suggests that Z-ISO could be regulated by NO *in vivo.* Further study of Z-ISO will be critical for advancing our limited understanding of post-translational regulation of carotenogenesis.

Hemoproteins possess a wide range of biological functions, as enzymes, electron transporters, gas sensors, gas transporters, and as transcription factors, but double-bond isomerization is not generally considered a prototype activity for hemoproteins[46]. Z-ISO is the only known heme-dependent isomerase that utilizes a ferrous iron, undergoes redox-mediated ligand switching, and performs isomerization of a long hydrocarbon in a membrane environment. Therefore, studies of Z-ISO as presented here open the path for further discovery and understanding of a new class of hemoenzymes that perform double-bond isomerization in hydrophobic environments. In the case of Z-ISO, isomerization is critical for mediating metabolic flux of a vital plant pathway that is also of importance for human and animal nutrition. Further understanding of Z-ISO function will provide opportunities to better control carotenoid biosynthesis for breeding more resilient plants in a changing climate and to facilitate production of more nutritious crops.

ONLINE METHODS

General gene cloning

All gene constructs were verified by DNA sequencing.

Z-ISO expression and purification

Cloning—The maize Z-ISO coding sequence with transit sequence was commercially synthesized (Genscript, Piscataway, NJ) to be codon optimized for *E. coli* and restriction sites added for cloning into *Sac*I and *Bam*H1 sites of pUC57 (see sequences in Supplementary Fig. 9). The final construct was named ZmZISO ACA-less (# 516). From this clone, the sequence encoding Z-ISO beginning at residue 49 was PCR amplified using primers (forward) tacttccaatccaatgccatg CGTCCGGCGCGTGCGGTGG and (reverse) TTATCCACTTCCAATG CTACCAGGGAAGTTGGTAGCTG and inserted by ligation

independent cloning (LIC) [47] into pMCSG9-10xHis (# 646). Primer sequences in lower case letters were for LIC cloning and those in uppercase were gene-specific. The resulting construct, pMCSG9 Z-ISO E2 (# 582), encodes a MBP::Z-ISO fusion protein consisting of a 10x-His-tagged maltose binding protein (MBP) at the N-terminus which is separated from the C-terminal Z-ISO by a TEV protease cleavage site. The pMCSG9-10xHis vector was produced by modifying vector pMCSG9 [48] and obtained from the materials repository of the Protein Structure Initiative [49] to have a 10x His tag instead of a 6xHis tag.

Expression and purification of the MBP::Z-ISO fusion protein—*E. coli* C43 (DE3) overnight cultures harboring pMCSG9 Z-ISO E2 (# 582) were used to inoculate 2 X YT medium (1% yeast extract, 1.6% tryptone and 0.5% NaCl) at 1:100 dilution. Cultures were incubated with shaking at 200 rpm at 37°C until an O.D. of 0.6 (typically ~2 h). Protein expression was induced with 1 mM isopropyl-1-thio-D-galactopyranoside (IPTG, Gold Biotechnology) and further incubated for 16 h at 28°C. Cultures were centrifuged at 2,600 x g for 15 minutes at 4°C and pellets frozen until use. Pellets were resuspended (at a ratio of 50 mL per 8 g of cell pellets, (~ 40 mL per liter of initial culture) in Resuspension Buffer (50 mM Tris pH 7.6 [Sigma-Aldrich], 300 mM NaCl, and 5% glycerol) containing 0.5 mM dithiothreitol (DTT, VWR), 4 μL/25 mL benzonase, (Sigma-Aldrich) and 60 mg/50 mL of 4-(2-Aminoethyl) benzenesulfonyl fluoride hydrochloride (AEBSF, Bio-Research Products) and 0.15 mg/mL of lysozyme (Sigma-Aldrich) before sonication on ice (5 times, 30 sec each, 60% power) using a Vibra Cell VC600 sonicator equipped with a 3 mm tapered microtip (Sonics & Materials Inc, Connecticut, USA) To remove unbroken cells, the preparations were centrifuged at ~15,000 x g (11,000 rpm in a Type 45 Ti rotor) for 15 minutes at 4 °C. To recover the membrane fraction, the supernatants were next centrifuged at ~120,000 x g (32,000 rpm in a Type 45 Ti rotor) for 1 h at 4 °C. The pellets containing cell membranes were resuspended in Resuspension Buffer at a ratio of 8 mL per liter of initial cell culture, following by sonication as described above. Following sonication, the volumes were increased for a total of 40 mL per liter of starting culture. n-Dodecyl β-D-maltoside (DDM [Anatrace]), added as powder was added to a final concentration of 1.5%. Samples were rotated end over end at 4°C for 15 min. Cleared lysates were incubated overnight with Ni-NTA containing resin (Qiagen) at a ratio of 300 μL resin per 40 mL of lysate for Immobilized Metal Affinity Chromatography (IMAC) in a 5 mL polypropylene column (Qiagen). The column was washed with five resin volumes of ATP Wash Buffer (40 mM Tris pH 7.6, 200 mM NaCl, 5% glycerol, and 5 mM $MgCl_2$), containing freshly added final concentrations of 5 mM ATP (Fisher Scientific), 0.1 mM DTT and 0.05% DDM for 30 min (column under gentle rotation). A second wash (5 resin volumes) with Wash Buffer (40 mM Tris pH 7.6, 400 mM NaCl, 5% glycerol) containing 0.1 mM DTT, 0.05% DDM and 30 mM histidine (Sigma-Aldrich) was performed for 5 min (column under gentle rotation). The MBP::Z-ISO fusion protein was eluted with Elution Buffer (25 mM Tris pH 7.6, 200 mM NaCl, 200 mM histidine and 5% glycerol) containing 0.1 mM DTT and 0.05% DDM at a ratio of 1 mL Elution Buffer per liter of initial culture. The protein sample was then dialyzed overnight using a Slide-A-Lyzer Dialysis cassette G2 20 K membrane,(Thermo-scientific, IL, USA) against 1000-fold volume of buffer containing 20 mM NaCl, 20 mM Tris (pH 7.6), 5% glycerol, 0.02% DDM, and 0.1 mM DTT at 4°C. For metal analysis, 1 mM EDTA was included in the dialysis buffer and dialysis was done for 3 h, three times. When needed,

the sample was concentrated using micro-concentrators (Microcon micro-concentrators 100 K, Amicon, Inc., Beverly, MA USA). For *in vitro* assays, protein was stored at −20°C in buffer containing 20 mM NaCl, 20 mM Tris (pH 7.6), 40% glycerol, 0.02% DDM, and 0.1 mM DTT. The yield of fusion protein was ~1 mg/liter culture at ~90% purity.

Expression and purification of NnrU—NnrU from *Agrobacterium tumefaciens* C58, was cloned in pNYCOMPS[49] as a C-terminal fusion to a TEV protease cleavage site and a 10x His tag (NnrU C1, # 744), expressed in *E. coli* and purified as described above for Z-ISO.

Z-ISO *in vitro* enzyme assay

Preparation of substrate-containing liposomes—To produce the substrate, 9,15,9′-tri-*cis*-ζ̃carotene (tri) from *E. coli* BL21 (DE3) cultures, 400 mL of Luria-Bertani (LB) medium (1% tryptone, 0.5% yeast extract, and 1% NaCl) containing chloramphenicol (34 μg/mL [Sigma-Aldrich]) was inoculated with 8 mL of overnight culture containing pACCRT-EBP (#150). Cultures were grown in the dark at 37°C, with shaking at 160 rpm for 8 h before induction with 10 mM IPTG. Cultures were further incubated at 28°C, with shaking at 100 rpm for 40 h and an additional 2 d without shaking. Cells were centrifuged at 2,600 x g and pellets were resuspended in a total of 40 mL of methanol, distributed in 4 Falcon tubes with equal volumes of extract and sonicated twice on ice, for 30 sec each at 60% power using a Vibra Cell VC600 sonicator equipped with a tapered 3 mm microtip (Sonics & Materials Inc, Connecticut, USA). Extracts were centrifuged at 2,600 x g for 10 min and supernatants were transferred to 15 mL Falcon tubes and evaporated under nitrogen gas in the dark. Dried samples were resolubilized in 300 μL of methanol, transferred to 1.5 mL microfuge tubes, frozen at 80°C for 1 h and centrifuged at 16,000 x g at 4°C. Extractions were then combined and 1 mL used to prepare liposomes. Cells also accumulate 9,9′-tri-*cis*-ζ-carotene (di) and therefore enzymatic conversion is measured as the ratio of di to tri isomers. To prepare liposomes, one mL of substrate extract (58 μM, estimated by spectroscopy using the molar extinction coefficient for ζ-carotene [50]; ε_{400} = 138,000) was mixed with 35 μL of soybean L-α-Phosphatidylcholine (Sigma-Aldrich, 99% pure) (20 mg/mL in methanol). The mixture was dried under N_2 followed by addition of 800 μL sonication buffer (25 mM HEPES pH 7.8, 100 mM NaCl, 10% glycerol) and sonicated on ice using a Vibra Cell VC600 sonicator equipped with a 3 mm tapered microtip (Sonics & Materials Inc, Connecticut, USA) for 1 min at intervals of 10 s at 20% power.

***In vitro* reactions—**To assemble a biphasic assay system (final volume of 400 μL), purified, MBP::Z-ISO fusion protein (10 μM final concentration) was incubated with 15 μL of AcTEV protease (150 units, Invitrogen) for 2 min at RT. To generate reducing conditions, freshly prepared sodium dithionite (Sigma-Aldrich, 85% pure) was added to a final concentration of 10 mM in the assay. To initiate the reaction, 200 μL of substrate-containing liposomes, (for a final concentration of 36.5 μM substrate) were added and reactions were overlaid with N_2 gas before capping. Reactions were incubated at 28°C under continuous shaking at 130 rpm for 3 h in the dark (to prevent photoisomerization). Reactions in the absence of sodium dithionite were also assembled. As a negative control, heat denatured (10 min at 100°C) MBP::Z-ISO fusion was used. Reactions were extracted by addition of 1 mL

of petroleum ether/diethyl ether 2:1 (v/v) and the organic phase collected, dried under N_2, dissolved in 150 μL methanol and 100 μL separated by HPLC as described below. All reactions were replicated three times.

Bioinformatics

MEMSAT3[7], which has been experimentally validated as one of the better predictors of membrane topology, [51] was used to predict transmembrane domains in maize Z-ISO. The transit peptide sequence was predicted using the ChloroP program as reported [3]. The Z-ISO protein sequence from *Zea mays*[3] was analyzed by the fold-recognition program, LOOPP (LOOPP parallel driver v7.0 with LOOPP v3.20)[11] which modeled 276 residues of Z-ISO onto a di-iron protein, Protein Databank structure 2INP. The resulting model is shown in Figure 6a. The alignment of the two sequences is shown in Supplementary Fig. 10.

HPLC Analysis

HPLC separations were performed on a Waters HPLC system equipped with a 2695 separation module, 996 photodiode array detector (Waters), and Empower I software (Waters). A C30 Develosil 5u RPAQUEOUS (250 x 4.6 mm) column from Phenomenex (Nomura Chemical Co. Ltd, Seto, Japan) was used. For isocratic separation of 100 μL of carotenoid extract, a mobile phase of four parts water, 66 parts methanol (VWR, HPLC grade), and 30 parts methyl-t-butyl-ether (VWR, HPLC grade) at a constant flow rate of 1 mL/min for 80 min was applied. Identification of ζ-carotene isomers was based on elution time and spectra as published [3].

Z-ISO Localization

Transient expression of Z-ISO in protoplasts—A full copy of maize Z-ISO without a stop codon was amplified from pColZmZ-ISO1 plasmid (#497) [3], with forward primer 2793 (*5′atctctagaATGGCCTCCCAGCTCCGCCTCCACC*), containing an *Xba*I site, and reverse primer 2794 (*5′atcggatccCCAGGGAAGTTGGTAGCTGGATGC*), containing a *Bam*HI site, and inserted into the pUC35S-sGFP-Nos vector [52] (digested with *Xba*I/*Bam*HI), to produce the pUC35S-M-ZISO-sGFP-Nos plasmid (#568) which was used for transient expression. Transient expression of Z-ISO-GFP in maize green leaf protoplasts was performed as described [52].

In vitro import of Z-ISO into chloroplasts—A full copy of the maize Z-ISO gene, without a stop codon, was amplified from pColZmZ-ISO1 (#497) [3] using forward primer 2851 (*ccacctgcaGAATTCtatggcctc*), containing an *Eco*RI site, and reverse primer 2854 (*gtcTCTAGAttatttttcaaattgaggatgagaccaccagggaagttggtagct*), containing a Strep-tag and XbaI site, and inserted into vector pTnT (Promega), which was digested with the same restriction enzymes, to yield plasmid pTnT-M-ZISO-Strep (#570). pTnT-M-ZISO-Strep was used as a template for *in vitro* protein synthesis. *In vitro* protein synthesis and import of Z-ISO into isolated pea chloroplasts were performed as described [52]. After import, chloroplasts were treated with thermolysin (+) to remove nonspecifically bound protein. Chloroplasts were also fractionated into soluble (S) and membrane (M) fractions, including envelope and thylakoid; an equal amount of the membrane fraction as in M was alkaline-treated (MA) to remove peripheral membrane proteins indicating Z-ISO is a membrane integral protein. We

previously showed that alkaline treatment will remove loosely associated peripheral membrane proteins as compared to integral membrane proteins which remain membrane associated [52,53]

Identification of a Z-ISO complex—After ^{35}S-met-labelled Z-ISO was imported into chloroplasts, the chloroplast sample was treated with 0.5% Triton X-100 to isolate protein complexes under native conditions. The sample was then separated into individual complexes by native gel electrophoresis in a NativePAGe Novex 4–16% gel (Invitrogen, Life Technologies), following the instructions of the manufacturer. The gel was then dried and the radioactive band detected by a Phosphorimager system (Amersham, GE Life Sciences). The size of the band was estimated in comparison to NativeMark protein marker (Invitrogen, Life Technologies).

Detection of metals in Z-ISO

Inductively Coupled Plasma Optical Emission Spectrometry (ICP-OES)—Samples of MBP:: Z-ISO (>90% pure) were dialyzed three times each against 1000 fold buffer (20mM Tris pH 7.6, 20mM NaCl, 5% glycerol, 0.02% DDM, 0.1 mM DTT and 1mM EDTA) and injected into a Spectro Genesis inductively-coupled optical emission spectrometer (ICP-OES) to measure the concentrations of iron at 238.204 nm and 259.941 nm and sulfur at 180.731 nm, as previously described [54]. For 23 μM protein, 15.4 μM Fe was detected. Levels of Ca, Cu, Ni, Mg, Mn, Mo or Zn were insignificant.

Detection of heme

Pyridine hemochrome assay—To determinate whether the chromophore bound to Z-ISO was heme, a pyridine hemocrome assay was performed [55]. Purified protein (750 μL) was mixed with 75 μL of 1 N NaOH (Fisher Scientific), 175 μL of pyridine (Sigma-Aldrich) and 2 mg of sodium dithionite. The UV-visible absorption spectrum was immediately recorded and compared with the spectrum of the initial purified sample before addition of dithionite. The presence of the Soret band at 414 nm in the ferric state and the presence of the Soret band (418 nm) and appearance of the α/β bands at 555 and 530 nm respectively in the ferrous state were used as evidence for the presence of heme.

Heme stain—Heme staining, based on heme peroxidase activity, was performed essentially as reported [56]. Protein samples were separated on a NuPAGE® Bis-Tris 12% polyacrylamide gel (Invitrogen). The gel was rinsed with water for 15 s and then incubated for 1 h in the dark in a solution containing 30 mL of 40 mM TMBZ (3,3,5,5′-Tetramethylbenzidine, Sigma-Aldrich) in methanol followed by the addition of 70 mL of 0.25 M sodium acetate pH 5.0 (Sigma-Aldrich). Then, 5 mL of 3% hydrogen peroxide were added and mixed well until a signal corresponding to the MBP Z-ISO band appeared. The gel background was removed by destaining 15 min with 3:7 isopropanol: 0.25 M sodium acetate.

Binding of CN^-

MBP::Z-ISO, 75.46 KDa (1.58 mg/ml, 21 μM), purified as described above, was incubated with KCN (Sigma-Aldrich, ≥96% pure) at a final concentration of 2 mM. The UV visible

spectrum was recorded before and immediately after addition and mixing of KCN. The experiment was repeated except that MBP::Z-ISO was first reduced with sodium dithionite (2 mg, added as dry powder) before addition of KCN.

UV-Visible Spectroscopy (UV-Vis) Z-ISO difference spectra

In the reduced *minus* oxidized spectrum (Fig. 2d), the graph was obtained by subtracting the UV-Vis spectrum of the dithionite-reduced enzyme from the spectrum of the enzyme as-purified. In the CO difference spectrum (Fig. 2d), the graph was obtained by subtracting the UV-Vis spectrum of the dithionite-reduced enzyme from the spectrum of the enzyme which was dithionite-reduced and then treated with CO. For the CN^- difference spectra, the graph was obtained by subtracting the UV-Vis spectrum of the as-purified enzyme from the spectrum of the as-purified enzyme which was treated with CN^- (Fig. 2e inset), or by subtracting the UV-Vis spectrum of the dithionite-reduced enzyme from the spectrum of the dithionite-reduced enzyme which was treated with CN^- (Supplementary Fig. 6).

Electron spin resonance (EPR) spectroscopy

X-band EPR spectra of Z-ISO were recorded in the perpendicular mode on a Bruker ER200D spectrometer coupled with a 4116DM resonator at 100 kHz modulation frequency. The measurement temperature was maintained at 10 K using an ESR910 liquid helium cryostat and an ITC503 temperature controller from Oxford Instrument (Concord, MA). The reduced Z-ISO protein was generated by dithionate reduction under anaerobic conditions. Nitric oxide (NO) was anaerobically introduced through a gas-tight syringe to the headspace of the quartz EPR tubes containing reduced Z-ISO. An argon flush was maintained above samples to protect them from oxidation by O_2 and to minimize an anomalous EPR signal near $g = 2$ which derives from NO.

Magnetic Circular Dichroism (MCD)

MCD spectra were measured on a Jasco J815 spectropolarimeter fitted with a Jasco MCD-1B magnet at a magnetic field strength of 1.41 T at 4°C using a 0.5 cm pathlength quartz cuvette and interfaced with a Silicon Solutions PC through a JASCO IF-815-2 interface unit. MCD data acquisitions and manipulations were carried out using JASCO software as reported previously[57].

Site-directed mutagenesis and functional complementation in *E. coli*

The maize Z-ISO cDNA coding sequence from pColZmZ-ISO1 plasmid (#497) [3] was used as a template to PCR amplify and subclone Z-ISO lacking the transit peptide sequence (amino acids 1–46). For PCR, forward primer (5′ cgggatcctCACGCTCGTCCCGCCCGTGCG 3′) containing a *Bam*HI site and reverse primer (5′ gcgtcgaccTACCAGGGAAGTTGGTAGCT3′) containing a *Sal*I site were used. Lowercase letters in primers contain restrictions sites and uppercase letters contain gene specific sequences. The resulting PCR product was further inserted into the *BamH*I and *Sal*I sites of pCOLADuet-1 forming a His-tag::Z-ISO fusion and named pCola Zm Z-ISO NTP (#579). pCola Z-ISO NTP was then used as template to perform substitutions of conserved residues to Ala. Residue substitutions used in this study were: His-150 (#797, pCol Zm Z-

ISO NTP H150A), His-266 (#798, pCol Zm Z-ISO NTP H266A) and Cys-263 (#796, pCol Zm Z-ISO NTP C263A). Other residue substitutions tested were made in the pColZmZ-ISO1 plasmid (#497): His-191 (#523, pCol Zm Z-ISO H191A), His-208A (#528, pCol Zm Z-ISO H208A), His-241 (#529, pCol Zm Z-ISO H241A), His-253 (#530, pCol Zm Z-ISO H253A), His-354 (#532, pCol Zm H354A), His-285 (#525, pCol Zm H285A), H286A (#526, pCol Zm Z-ISO H286A). For H150, H266, and C263, mutations were also created in the MBP::Z-ISO fusion construct using the pMCSG9 Z-ISO E2 plasmid (#582) as template to generate the following MBP::Z-ISO mutant versions: pMCSG9 Z-ISO E2 H150A (#619), pMCSG9 Z-ISO E2 H266A (#620) and pMCSG9 Z-ISO E2 C263A (#801) which were expressed in *E. coli* as described above (see: Expression and purification of the MBP::Z-ISO fusion protein). Reactions for mutagenesis were performed using the Quick-change® Lightning Site-Directed Mutagenesis Kit (Stratagene) and primers designed to incorporate the desired substitution. For functional testing, the Z-ISO mutant genes were further transformed into *E. coli* cells harboring the plasmid pACCRT-EBP (#150) which confers accumulation of ζ-carotene [3]. For functional complementation, mutant Z-ISO genes were introduced into *E. coli cells* accumulating the Z-ISO substrate. Carotenoids were extracted from the bacteria harboring the various enzyme variants and subjected to HPLC analysis to quantify the ratio of product (di-*cis* which refers to 9,9′ di-*cis*-ζ-carotene) to substrate (tri-*cis* which refers to 9,15,9′ tri-*cis*-ζ-carotene). Cells with empty vector also accumulate a small amount of product. Therefore enzyme activity is judged by the increase over this background level. Specifically, 1 mL of saturated cultures in LB medium (1% tryptone, 0.5% yeast extract, and 1% NaCl) were added to 50 mL of fresh medium and then grown in the dark at 37°C at 200 rpm for 8h before induction with 10 mM IPTG and further incubation for 40 h at 28°C with slow shaking (100 rpm) and an additional 2 days without shaking. For carotenoid extraction, bacterial cultures were centrifuged at 2,600 x g for 10 min. Pellets were resuspended in 5 mL of methanol containing 1% of butylated hydroxytoluene (BHT, Sigma-Aldrich, ≥99% pure) and sonicated using a Vibra Cell VC600 sonicator equipped with a 3 mm tapered microtip (Sonics & Materials Inc, Connecticut, USA) on ice twice, 30 sec each, 60% power. Extracts were centrifuged at 2,600 x g for 10 min and supernatants were transferred to 15 mL Falcon tubes and extracts evaporated under nitrogen gas in the dark. Dried samples were resolubilized in 500 μL of methanol, transferred to 1.5 mL tubes, frozen at 80°C for 1 h, centrifuged at 16,000 x g at 4°C, and supernatants used for HPLC separation as described above. Complementation experiments were replicated three times.

Immunodetection of Z-ISO

For antibody generation, 2 mg of MBP::Z-ISO protein (#582) were digested with TEV protease to generate free Z-ISO. Samples were separated using the NuPAGE system from Invitrogen (Carlsbad, USA). Protein bands corresponding to Z-ISO were excised and shipped to Lampire Biological Laboratories (Coopersburg, PA) for rabbit immunization. Polyclonal antibodies against Z-ISO were generated in two rabbits identified as #190202 and #190203. For immunodetection, protein samples were separated by electrophoresis using the NuPAGE system (Invitrogen). Reducing conditions in the samples were generated with DTT (100 mM). Proteins were transferred onto nitrocellulose membranes (Optitran; Whatman, Dassel, Germany) using an electrophoretic transfer cell (Criterion Blotter, Bio-

Rad) at 20 V overnight, 4°C using 1 X transfer buffer (25 mM Tris, 192 mM glycine and 20% (v/v) methanol). The membranes were then incubated in blocking buffer [1X Phosphate Buffered Saline buffer (137 mM NaCl, 2.7 mM KCl, 8 mM Na_2HPO_4, and 2 mM KH_2PO_4), 3% Bovine Serum Albumin (BSA, Fisher Scientific) and 1% Tween 20 (Sigma-Aldrich)] for 1 h at RT, then for 1 h at RT with anti-Z-ISO polyclonal antibody (1:2000) produced in rabbit (#190203). After washing, the membranes were incubated with horseradish peroxidase (HRP)-conjugated goat anti-rabbit IgG (Invitrogen) for 1 h at RT and washed with 1 X PBS buffer containing 1% Tween 20 for 15 min followed by four additional washes of 5 min each. Immunoreactions were visualized with the Super Signal West Dura kit (Thermo Scientific). Fluorescent signals were captured using a G-box (Chemi XT4) from Syngene with Genesys V1. 3.1.0 Software.

Supplementary Material

Refer to Web version on PubMed Central for supplementary material.

Acknowledgments

We thank Dr. Wayne Hendrickson (Columbia University and Principal Investigator, NIH-PSI New York Consortium on Membrane Protein Structure), for helpful discussions and use of the New York Structural Biology Center facilities. We thank Dr. Masayori Inouye (UMDNJ) for valuable advice on codon optimization and Dr. Louis Bradbury (Lehman College and CUNY) for helpful discussions. ETW was funded by the National Institutes of Health (grant GM081160), City University of New York and Lehman College. ETW was also supported by travel funds from the Gordon Research Conferences to attend the Metals in Biology Gordon Research Conference, where ETW was able to initiate collaborations with heme experts Hosler, Liu, and Dawson through the much appreciated help from Harry Gray (Cal Tech). The New York Consortium on Membrane protein structure (BK and JL) was supported through funds obtained from the National Institutes of General Medical Sciences Protein Structure Initiative (PSI) program (grant GM095315). JHD was funded by the National Institutes of Health grant GM 26730; AL was funded by National Institutes of Health grant R01GM108988 and the Georgia Research Alliance Distinguished Scholar Program. CAD was funded by The New Zealand Institute for Plant and Food Research Limited, New Zealand.

LITERATURE CITED

1. Moise AR, Al-Babili S, Wurtzel ET. Mechanistic aspects of carotenoid biosynthesis. Chemical Reviews. 2014; 114:164–193. [PubMed: 24175570]
2. Wurtzel ET, Cuttriss A, Vallabhaneni R. Maize provitamin A carotenoids, current resources and future metabolic engineering challenges. Frontiers in Plant Science. 2012; 3:29. [PubMed: 22645578]
3. Chen Y, Li F, Wurtzel ET. Isolation and characterization of the Z-ISO gene encoding a missing component of carotenoid biosynthesis in plants. Plant Physiol. 2010; 153:66–79. [PubMed: 20335404]
4. Li F, Murillo C, Wurtzel ET. Maize *Y9* encodes a product essential for 15-*cis* zetacarotene isomerization. Plant Physiol. 2007; 144:1181–1189. [PubMed: 17434985]
5. Janick-Buckner D, O'Neal J, Joyce E, Buckner B. Genetic and biochemical analysis of the *y9* gene of maize, a carotenoid biosynthetic gene. Maydica. 2001; 46:41–46.
6. Tatusova TA, Madden TL. Blast 2 sequences- a new tool for comparing protein and nucleotide sequences. FEMS Microbiol Lett. 1999; 174:247–250. [PubMed: 10339815]
7. Jones DT. Improving the accuracy of transmembrane protein topology prediction using evolutionary information. Bioinformatics. 2007; 23:538–544. [PubMed: 17237066]
8. Shumskaya M, Wurtzel ET. The carotenoid biosynthetic pathway: Thinking in all dimensions. Plant Science. 2013; 208:58–63. [PubMed: 23683930]

9. Ginalski KEA, Fischer D, Rychlewski L. 3D-Jury: a simple approach to improve protein structure predictions. Bioinformatics. 2003; 19:1015–1018. [PubMed: 12761065]
10. Madej MG, Nasiri HR, Hilgendorff NS, Schwalbe H, Lancaster CRD. Evidence for transmembrane proton transfer in a dihaem-containing membrane protein complex. EMBO J. 2006; 25:4963–4970. [PubMed: 17024183]
11. Brinda Kizhakke V, et al. Building and assessing atomic models of proteins from structural templates: Learning and benchmarks. Proteins: Structure, Function, and Bioinformatics. 2009; 76:930–945.
12. Thomas PE, Ryan D, Levin W. An improved staining procedure for the detection of the peroxidase activity of cytochrome P-450 on sodium dodecyl sulfate polyacrylamide gels. Anal Biochem. 1976; 75:168–76. [PubMed: 822747]
13. Nygaard T, Liu M, McClure M, Lei B. Identification and characterization of the heme-binding proteins SeShp and SeHtsA of *Streptococcus equi* subspecies *equi*. BMC Microbiology. 2006; 6:82. [PubMed: 17007644]
14. Owens CP, Du J, Dawson JH, Goulding CW. Characterization of heme ligation properties of Rv0203, a secreted heme binding protein involved in *Mycobacterium tuberculosis* heme uptake. Biochemistry. 2012; 51:1518–31. [PubMed: 22283334]
15. Boffi A, Chiancone E, Takahashi S, Rousseau DL. Stereochemistry of the Fe(II)– and Fe(III)–cyanide complexes of the homodimeric *Scapharca inaequivalvis* hemoglobin. A resonance raman and FTIR study. Biochemistry. 1997; 36:4505–4509. [PubMed: 9109658]
16. Tsai AL, et al. Heme coordination of prostaglandin H synthase. Journal of Biological Chemistry. 1993; 268:8554–63. [PubMed: 8386163]
17. Geng J, Dornevil K, Liu A. Chemical rescue of the distal histidine mutants of tryptophan 2,3-dioxygenase. J Am Chem Soc. 2012; 134:12209–18. [PubMed: 22742206]
18. Zoppellaro G, et al. Review: Studies of ferric heme proteins with highly anisotropic/highly axial low spin (S = 1/2) electron paramagnetic resonance signals with bis-Histidine and histidine-methionine axial iron coordination. Biopolymers. 2009; 91:1064–1082. [PubMed: 19536822]
19. Zhong F, Lisi GP, Collins DP, Dawson JH, Pletneva EV. Redox-dependent stability, protonation, and reactivity of cysteine-bound heme proteins. Proceedings of the National Academy of Sciences. 2014; 111:E306–E315.
20. Smith AT, et al. Identification of Cys94 as the distal ligand to the Fe(III) heme in the transcriptional regulator RcoM-2 from *Burkholderia xenovorans*. Journal of Biological Inorganic Chemistry. 2012; 17:1071–1082. [PubMed: 22855237]
21. Enemark JH, Feltham RD. Principles of structure, bonding, and reactivity for metal nitrosyl complexes. Coordination Chemistry Reviews. 1974; 13:339–406.
22. Yonetani T, Yamamoto H, Erman JE, Leigh JS Jr, Reed GH. Electromagnetic properties of hemoproteins. V. Optical and electron paramagnetic resonance characteristics of nitric oxide derivatives of metalloporphyrin-apohemoprotein complexes. J Biol Chem. 1972; 247:2447–55. [PubMed: 4336375]
23. Sun J, Wilks A, Ortiz de Montellano PR, Loehr TM. Resonance Raman and EPR spectroscopic studies on heme-heme oxygenase complexes. Biochemistry. 1993; 32:14151–7. [PubMed: 8260499]
24. Vickery L, Nozawa T, Sauer K. Magnetic circular dichroism studies of low-spin cytochromes. Temperature dependence and effects of axial coordination on the spectra of cytochrome *c* and cytochrome *b*5. J Am Chem Soc. 1976; 98:351–7. [PubMed: 1438]
25. Vickery L, Nozawa T, Sauer K. Magnetic circular dichroism studies of myoglobin complexes. Correlations with heme spin state and axial ligation. J Am Chem Soc. 1976; 98:343–50. [PubMed: 173751]
26. Sono M, Dawson JH, Hall K, Hager LP. Ligand and halide binding properties of chloroperoxidase: peroxidase-type active site heme environment with cytochrome P-450 type endogenous axial ligand and spectroscopic properties. Biochemistry. 1986; 25:347–56. [PubMed: 3955002]
27. Dawson JH, Andersson LA, Sono M. Spectroscopic investigations of ferric cytochrome P-450-CAM ligand complexes. Identification of the ligand trans to cysteinate in the native enzyme. J Biol Chem. 1982; 257:3606–17. [PubMed: 6277939]

28. Li T, Bonkovsky HL, Guo JT. Structural analysis of heme proteins: implications for design and prediction. BMC Struct Biol. 2011; 11:13. [PubMed: 21371326]
29. Wouters J, et al. Catalytic mechanism of *Escherichia coli* isopentenyl diphosphate isomerase involves Cys-67, Glu-116, and Tyr-104 as suggested by crystal structures of complexes with transition state analogues and irreversible inhibitors. J Biol Chem. 2003; 278:11903–8. [PubMed: 12540835]
30. D'Angelo P, et al. Unusual heme iron-lipid acyl chain coordination in *Escherichia coli* flavohemoglobin. Biophys J. 2004; 86:3882–92. [PubMed: 15189885]
31. Crabtree, RH. The Organometallic Chemistry of the Transition Metals. John Wiley & Sons, Inc; 2005. Complexes of π-Bound Ligands; p. 125-158.
32. Pearson RG. Hard and soft acids and bases, HSAB, part II: Underlying theories. Journal of Chemical Education. 1968; 45:643.
33. Heipieper HJ, Neumann G, Kabelitz N, Kastner M, Richnow HH. Carbon isotope fractionation during cis-trans isomerization of unsaturated fatty acids in *Pseudomonas putida*. Appl Microbiol Biotechnol. 2004; 66:285–90. [PubMed: 15480634]
34. Williams PA, et al. Haem-ligand switching during catalysis in crystals of a nitrogen-cycle enzyme. Nature. 1997; 389:406–412. [PubMed: 9311786]
35. Geng J, Davis I, Liu F, Liu A. Bis-Fe(IV): nature's sniper for long-range oxidation. J Biol Inorg Chem. 2014; 19:1057–67. [PubMed: 24722994]
36. Richter AS, Grimm B. Thiol-based redox control of enzymes involved in the tetrapyrrole biosynthesis pathway. Frontiers in Plant Science. 2013; 4:371. [PubMed: 24065975]
37. Fanciullino AL, Bidel LPR, Urban L. Carotenoid responses to environmental stimuli: integrating redox and carbon controls into a fruit model. Plant, Cell & Environment. 2014; 37:273–289.
38. Davison PA. Overexpression of beta-carotene hydroxylase enhances stress tolerance in *Arabidopsis*. Nature. 2002; 418:203–206. [PubMed: 12110893]
39. Johnson MP, et al. Elevated zeaxanthin bound to oligomeric LHCII enhances the resistance of Arabidopsis to photooxidative stress by a lipid-protective, antioxidant mechanism. J Biol Chem. 2007; 282:22605–22618. [PubMed: 17553786]
40. Walter MH, Floss DS, Strack D. Apocarotenoids: hormones, mycorrhizal metabolites and aroma volatiles. Planta. 2010; 232:1–17. [PubMed: 20396903]
41. Li F, Vallabhaneni R, Wurtzel ET. *PSY3*, a new member of the phytoene synthase gene family conserved in the Poaceae and regulator of abiotic-stress-induced root carotenogenesis. Plant Physiol. 2008; 146:1333–1345. [PubMed: 18162592]
42. Gas E, Flores-Perez U, Sauret-Gueto S, Rodriguez-Concepcion M. Hunting for plant nitric oxide synthase provides new evidence of a central role for plastids in nitric oxide metabolism. Plant Cell. 2009; 21:18–23. [PubMed: 19168714]
43. Chang HL, Hsu YT, Kang CY, Lee TM. Nitric oxide down-regulation of carotenoid synthesis and PSII activity in relation to very high light-induced singlet oxygen production and oxidative stress in *Chlamydomonas reinhardtii*. Plant and Cell Physiology. 2013; 54:1296–1315. [PubMed: 23713096]
44. Khatsenko O. Interactions between nitric oxide and cytochrome P-450 in the liver. Biochemistry (Mosc). 1998; 63:833–9. [PubMed: 9721336]
45. Cooper CE. Nitric oxide and iron proteins. Biochimica et Biophysica Acta (BBA) - Bioenergetics. 1999; 1411:290–309. [PubMed: 10320664]
46. Munro, A.; Girvan, H.; McLean, K.; Cheesman, M.; Leys, D. Heme and Hemoproteins. In: Warren, M.; Smith, A., editors. Tetrapyrroles, Birth, Life and Death. Landes Bioscience; Austin, Texas, USA: 2009. p. 160-183.
47. Doyle SA. High-throughput cloning for proteomics research. Methods Mol Biol. 2005; 310:107–13. [PubMed: 16350949]
48. Donnelly MI, et al. An expression vector tailored for large-scale, high-throughput purification of recombinant proteins. Protein Expr Purif. 2006; 47:446–54. [PubMed: 16497515]
49. Seiler CY, et al. DNASU plasmid and PSI:Biology-Materials repositories: resources to accelerate biological research. Nucleic Acids Res. 2014; 42:D1253–60. [PubMed: 24225319]

50. Britton, G.; Liaaen-Jensen, S.; Pfander, H. UV/visible spectroscopy. In: Britton, G.; Liaaen-Jensen, S.; Pfander, H., editors. Carotenoids- Volume 1B: Spectroscopy. Birkhäuser; Basel: 1995. p. 13-62.

51. ter Horst R, Lolkema JS. Rapid screening of membrane topology of secondary transport proteins. Biochimica et Biophysica Acta (BBA) - Biomembranes. 2010; 1798:672–680. [PubMed: 19932679]

52. Shumskaya M, Bradbury LMT, Monaco RR, Wurtzel ET. Plastid localization of the key carotenoid enzyme phytoene synthase is altered by isozyme, allelic variation, and activity. The Plant Cell. 2012; 24:3725–3741. [PubMed: 23023170]

53. Quinlan RF, et al. Synergistic interactions between carotene ring hydroxylases drive lutein formation in plant carotenoid biosynthesis. Plant Physiol. 2012; 160:204–214. [PubMed: 22786888]

54. Varanasi L, Hosler JP. Subunit III-depleted cytochrome c oxidase provides insight into the process of proton uptake by proteins. Biochim Biophys Acta. 2012; 1817:545–51. [PubMed: 22023935]

55. Berry EA, Trumpower BL. Simultaneous determination of hemes a, b, and c from pyridine hemochrome spectra. Analytical Biochemistry. 1987; 161:1–15. [PubMed: 3578775]

56. Thomas PE, Ryan D, Levin W. An improved staining procedure for the detection of the peroxidase activity of cytochrome P-450 on sodium dodecyl sulfate polyacrylamide gels. Analytical Biochemistry. 1976; 75:168–176. [PubMed: 822747]

57. Pond AE, Roach MP, Thomas MR, Boxer SG, Dawson JH. The H93G myoglobin cavity mutant as a versatile template for modeling heme proteins: ferrous, ferric, and ferryl mixed-ligand complexes with imidazole in the cavity. Inorg Chem. 2000; 39:6061–6. [PubMed: 11151505]

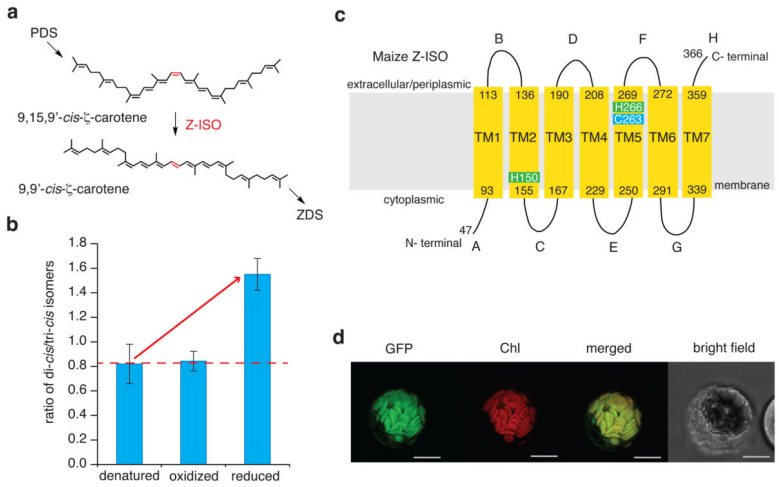

Figure 1. Z-ISO is an isomerase and integral membrane protein localized to chloroplasts

(**a**) Steps are shown in the carotenoid biosynthetic pathway where Z-ISO catalyzes the *cis* to *trans* isomerization of the central 15–15′ C-C double bond of 9,15,9′-tri-*cis*-ζ-carotene (tri-*cis*), the product of PDS, to form 9,9′-di-*cis*-ζ-carotene (di-*cis*), the substrate of ZDS. (**b**) Z-ISO *in vitro* enzymatic assay using substrate-containing liposomes and purified MBP::Z-ISO fusion protein. To initiate the reaction, substrate-containing liposomes (with a starting ratio of ~0.8 di-*cis*/tri-*cis* isomers as indicated by the red dashed line) were added and incubated in the dark. Conversion of substrate to product as measure by HPLC is seen as an increase in the ratio of 9,9′-di-*cis*-ζ-carotene/9,15,9′ tri-*cis*-ζ-carotene over background levels. To generate reducing conditions for the reduced/active enzyme and heat denatured/inactive enzyme, freshly prepared sodium dithionite was added in the assay to a final concentration of 10 mM. The as-purified enzyme was already “oxidized” and the reaction did not contain sodium dithionite. Data represent mean values ± s.d. for three 3 replicates. (**c**) Maize Z-ISO topology predicted by MEMSAT3. The N-terminal transit sequence (1–46) predicted by ChloroP is not shown.TM, transmembrane domain; letters and numbers denote loops and residues, respectively. Residues discussed in this paper are highlighted. (**d**) Z-ISO transiently expressed in maize leaf chloroplasts as a GFP fusion protein was co-localized with chlorophyll as seen in rightmost panel of merged signals from green GFP (Z-ISO) and red chlorophyll autofluorescence observed in a single cell. Bar=10 μm.

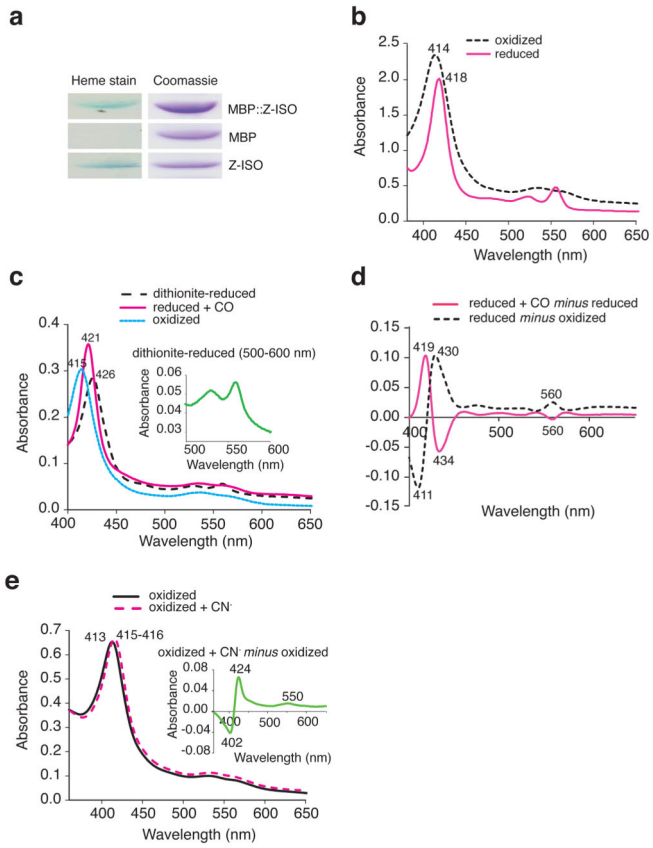

Figure 2. Z-ISO contains heme iron

(**a**) MBP::Z-ISO was cleaved with TEV protease to release Z-ISO and MBP which were separated by SDS-PAGE and either stained for heme or by Coomassie for protein. Only individual bands are shown. See Supplementary Figure 4 for uncut gel images. (**b**) UV-visible absorption spectrum from a pyridine hemochrome assay of Ni-affinity purified MBP::Z-ISO protein extract (Blue: resting; Red: reduced). (**c**) UV-Vis spectrum of MBP::Z-ISO which was as isolated (oxidized), dithionite-reduced, or dithionite-reduced and treated with carbon monoxide (CO). Absolute reduced spectrum: α band max= 559 nm. Soret (g) max = 426 nm; α/g=10.7. The inset shows an expanded view of the 500–600 nm region. (**d**) the difference spectrum of data taken from (**c**). (**e**) Binding of CN^- (2 mM) to as-purified Z-ISO(21 μM). The inset shows the difference spectra. See Supplementary Fig. 6 showing spectra from CN^- binding to the dithionite-reduced enzyme.

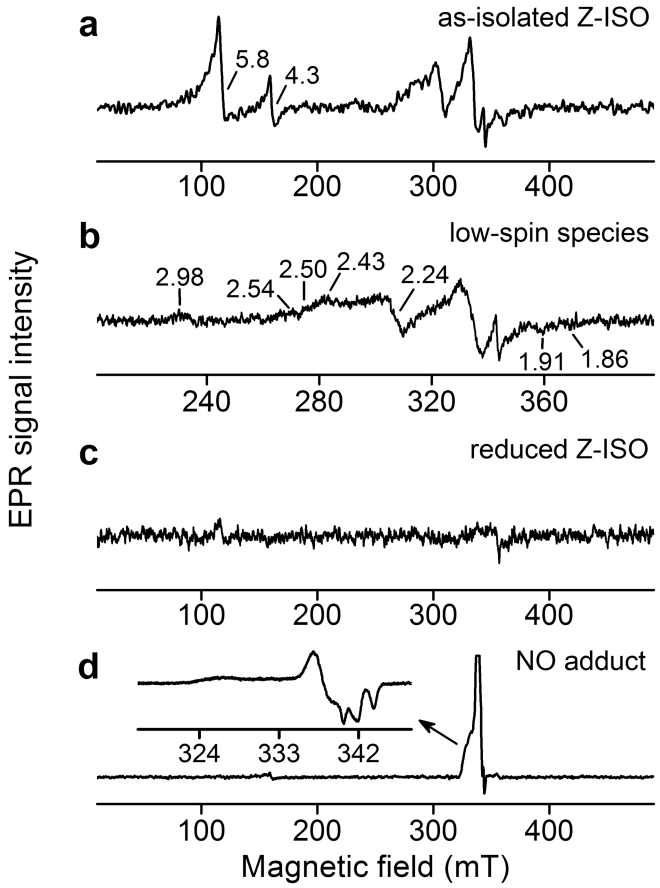

Figure 3. EPR shows multiple heme species

(**a**) EPR spectrum of as-purified Z-ISO. (**b**) A zoom-in view of the low-spin region of (**a**). (**c**) EPR spectrum of dithionite-reduced Z-ISO. (**d**) EPR spectrum of reduced Z-ISO further treated with NO. The inset shows a zoom-in view of the nitrosyl adduct of Z-ISO.

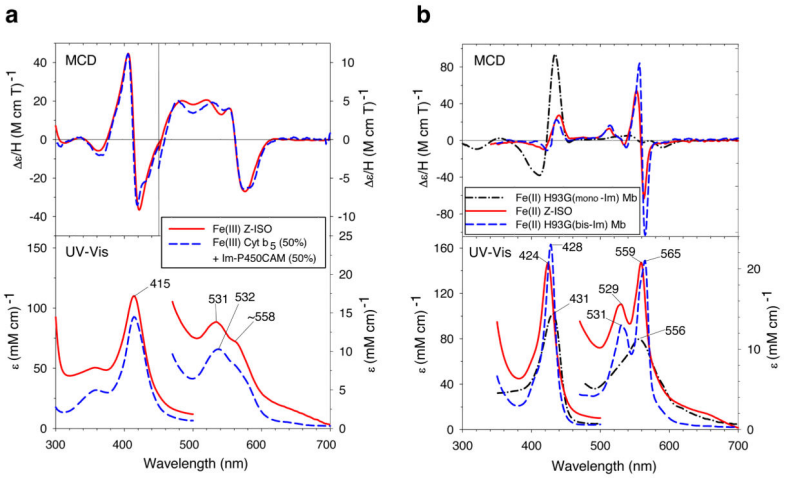

Figure 4. MCD reveals redox-dependent changes in ligand coordination

(**a**) MCD spectrum of as-purified Fe(III) Z-ISO (oxidized) is compared with a 50/50 mixture of Fe(III) Cyt. b_5 (bis-His) and Imidazole (Im)-bound Fe(III) $P450_{CAM}$ (His-Cys). (**b**). MCD spectrum of dithionite-reduced ferrous [Fe(II)] Z-ISO as compared with spectra of mono and bis Im- bound H93G Mb.

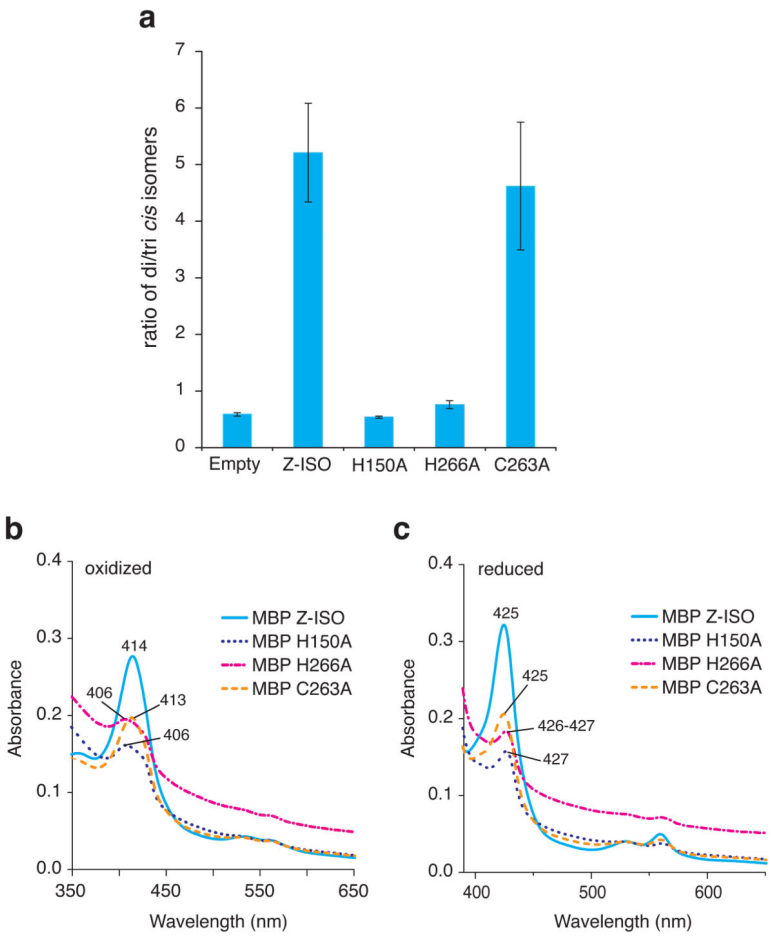

Figure 5. Testing mutation of putative heme ligands on enzyme activity, heme binding and UV-Vis spectrum of Z-ISO

(**a**) Isomerization activity was tested by functional complementation in *E. coli* and carotenoid products measured by HPLC. H150A and H266A were inactive and no different than the empty vector control. C263A retained activity similar to the nonmutant Z-ISO. Data represent mean values ± s.d. for three replicates. (**b**) and (**c**), UV-Vis spectra normalized for absorbance at 280 nm for extracted mutant fusion proteins which were as-purified (**b**) or dithionite-reduced (**c**). Peak maxima are listed in Supplementary Table 3.

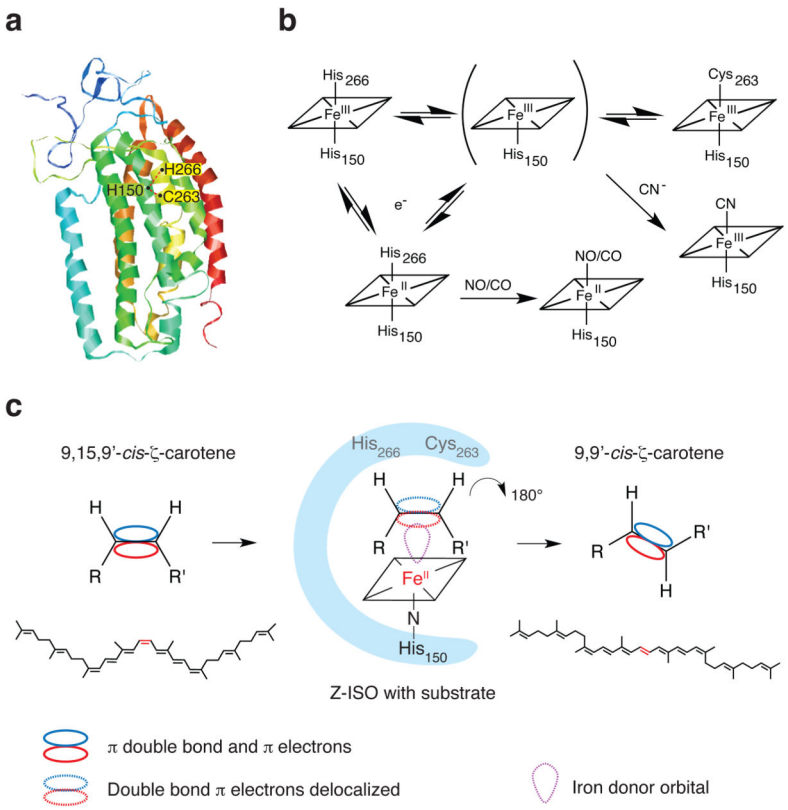

Figure 6. Proposed mechanism of ligand rearrangement leading to active isomerization

(**a**) Proximity of alternate heme ligands as seen in the Z-ISO homology model predicts feasibility of distal ligand switching between H266 and C263 where the heme proximal ligand is H150. (**b**) Proposed heme ligand states based on experimental evidence. Alternate ligands states for the Z-ISO heme (His-His or His-Cys) were predicted from the MCD and EPR data. Diagnostic probes, NO, CO, CN^-, were used to reveal specific states of the as-purified or dithionite-reduced enzyme. Cyanide (CN^-) was used to capture the high spin mono-ligated intermediate. Binding of NO and CO to Z-ISO revealed available coordination sites on the heme originating from a weakly bound distal ligand. (**c**) Model for Z-ISO isomerization. The Fe(II) in the Z-ISO heme coordinates its electrons with the delocalized π electrons (shaded) of the 15–15′ *cis* C=C bond of 9, 15, 9′-ζ-carotene. The resulting carbon-carbon bond becomes single bond in character and therefore is able to rotate to the thermodynamically favorable *trans* orientation.